

Engineering Notes

Numerical Validation of an Effective Radiation Heat Transfer Model for Fiber Preforms

A. J. van Eekelen*

SAMTECH, B-4031 Liège, Belgium
and

J. Lachaud†

University of California,
Santa Cruz, Moffett Field, California 94035

DOI: 10.2514/1.51865

Nomenclature

A_i	=	surface, m ²
c	=	capacity, J/(kg.K)
d	=	distance, m
F_{ij}	=	view factor, -
H_i	=	incident flux, W/(m ²)
k	=	correlation coefficient, -
\bar{k}	=	average correlation coefficient, -
q	=	heat flux, W/(m ²)
R_i	=	radiosity, W/(m ²)
T	=	temperature, K
Δx	=	length of the model, m
Δy	=	height of the model, m
Δz	=	depth of the model, m
ϵ_σ	=	emissivity, -
ρ	=	density, kg/(m ³)
λ	=	conductivity, W/(m.K)
σ	=	Stefan–Boltzmann constant, $5.67 \cdot 10^{-8}$ W/(m ² .K ⁴)
σ_{ext}	=	specific extinction coefficient, m ² /kg

Subscripts

0	=	apparent value
1, 2	=	walls
i	=	fiber faces
r	=	radiative
λ	=	conductive

I. Introduction

RADIATIVE heat transfer in fibrous materials has been the subject of numerous investigations [1–5]. Models with different degree of complexity and accuracy have been proposed. They range from semi-analytical models anchored by experimental

Presented as Paper 2010-4904 at the 10th AIAA/ASME Joint Thermophysics and Heat Transfer Conference, Chicago, IL, 28 June–1 July, 2010; received 2 August 2010; revision received 5 January 2011; accepted for publication 11 January 2011. Copyright © 2011 by the American Institute of Aeronautics and Astronautics, Inc. All rights reserved. Copies of this paper may be made for personal or internal use, on condition that the copier pay the \$10.00 per-copy fee to the Copyright Clearance Center, Inc., 222 Rosewood Drive, Danvers, MA 01923; include the code 0022-4650/11 and \$10.00 in correspondence with the CCC.

*Product Manager, Analysis Department, Rue des Chasseurs-Ardennais 8. Member AIAA.

†Associate Scientist, UARC, NASA Ames Research Center, Mail Stop 230-3.

data [6], to an accurate analytical modeling of the radiative energy transport through an absorbing and scattering medium [3]. The later method gives excellent results but counts two major drawbacks:

1) It is limited to materials with an homogeneous distribution of well-defined geometrical features (e.g., spheres, cylinders).

2) It is not practical to implement in macroscopic material-response simulation tools.

This study has two complementary short term objectives [with long-term goals noted between brackets]:

1) Extend the applicability of ab-initio methods, with the development of a direct numerical simulation (DNS) tool allowing the treatment of any geometry. [The long-term goal is to compute material properties from three-dimensional material-architecture reconstruction obtained by computed X-ray microtomography.]

2) Develop an effective radiative transfer model for thin layers of two-dimensional low-density carbon-fiber preforms, that may be integrated in macroscopic material-response tools. Perform a DNS analysis and validate the effective radiative transfer model. [The long-term goal is to generalize the validation or extend the model to any architecture.]

The article is organized as follows. In the second section, the material properties are discussed, an effective conductivity model is derived, and the DNS approach is presented. In the third section, the parameters of the effective model are obtained from steady-state DNS. In the fourth section, the accuracy of the effective model in the transient regime is compared to time-accurate DNS.

II. Model and Simulation Tool

A. Material Model and Problem Studied

In this first study, we shall consider that the carbon-fiber preform is two-dimensional with fibers parallel to each other. The following carbon-fiber properties, representative of literature data, will be used: conductivity, $\lambda = 10$ W/(m.K); specific heat capacity, $c = 1000$ J/(kg.K); density, $\rho = 1800$ kg/m³; and emissivity, $\epsilon_\sigma = 0.85$ (gray body). The fibers are treated as perfect cylinders with a diameter of 10 μ m. The fiber volume fraction of carbon-fiber preform is typically about 0.1. The model material for the DNS is generated using a Monte–Carlo procedure: nonoverlapping fibers are randomly placed in a rectangular box until the required volume fraction is obtained (Fig. 1). Therefore, the model is heterogeneous and two-dimensional at the microscopic scale, and homogeneous isotropic at the macroscopic scale.

We shall study the problem of Deissler [7]; that is, we shall assume that there are imaginary walls on the right hand side and on the left-hand side of the box containing the fibers (Fig. 1), with equal emissivities ϵ_σ for both walls and for the fibers. The model is taken periodic in the y -direction. The macroscopic problem is then one dimensional.

B. Effective Radiative Transfer Model

The diffuse gray radiation model between two infinite parallel planes may be linearized (Fourier's form) and the effective radiation conductivity λ_r can be written as:

$$\lambda_r = \frac{k\epsilon_\sigma}{2 - \epsilon_\sigma} \sigma T^3 \Delta x \quad (1)$$

where $k = 4$, is a geometric factor. In the presence of fibers, the value of k is modified.

Under the hypothesis of Rosseland (optically thick medium), the effective conductivity may be expressed as a function of the emissivity ϵ_σ and the thickness of the model Δx [6]:

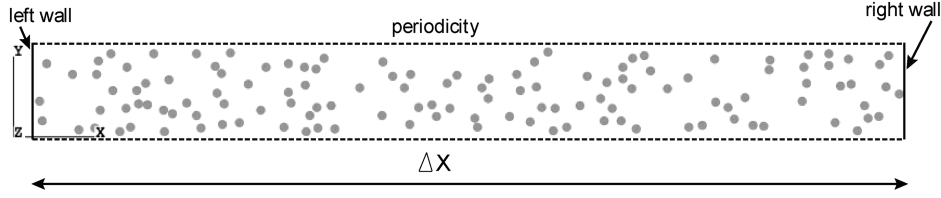


Fig. 1 Random distribution of fibers between two walls ($\Delta x = 1$ mm).

$$\lambda_r = \frac{4\epsilon_\sigma \sigma T^3 \Delta x}{(2 - \epsilon_\sigma) + \sigma_{\text{ext}} \epsilon_\sigma \rho_0 \Delta x} \quad (2)$$

where ρ_0 is the effective density of the material and σ_{ext} is the specific effective extinction coefficient that must be obtained for a given fiber configuration. Combining Eqs. (1) and (2), the geometric factor k for the fibrous medium may be expressed a function of Δx as

$$k = \frac{4(2 - \epsilon_\sigma)}{(2 - \epsilon_\sigma) + \sigma_{\text{ext}} \epsilon_\sigma \rho_0 \Delta x} \quad (3)$$

The radiation heat flux q_r may be written as

$$q_r = -\frac{k\epsilon_\sigma}{2 - \epsilon_\sigma} \sigma T^3 \Delta x \frac{\Delta T}{\Delta x} = -\frac{k\epsilon_\sigma}{2 - \epsilon_\sigma} \sigma T^3 \Delta T \quad (4)$$

C. Ab-Initio Physical Model and Associated DNS Tool

An electromagnetic wave or photon passing through the immediate vicinity of a fiber is either absorbed or scattered. The scattering is due to three separate phenomena, namely, 1) diffraction (waves never come into contact with the fiber, but their direction of propagation is altered by the presence of the fiber), 2) reflection (waves reflected from the surface of the fiber), and 3) refraction (waves that penetrate the fiber and, after partial absorption, reemerge traveling in a different direction) [8]. Carbon fibers are opaque, therefore, there is no refraction. The carbon-fiber surface is rough, generating a diffuse reflection. Diffraction is critical when the wavelength is not small compared with the fiber diameter. In the case of fibrous media, the size parameter x is defined as:

$$x = \frac{d \cdot \pi}{\lambda} \quad (5)$$

where the fiber diameter d equals $10 \mu\text{m}$ and where λ is the wavelength of interest. In general, diffraction is negligible for $x \geq 10$ [8]. However, the work of Lee [1] has shown that diffraction, for randomly oriented fibers, has a negligible effect on effective heat transfer for values of x larger than unity. Hence, diffraction may be neglected for wavelengths smaller than $\lambda_{\text{lim}} = 31.4 \mu\text{m}$. According to Plank's law, 99% of the energy of a black (or gray) body is emitted at wavelengths smaller than $\lambda_{\text{lim}} = 31.4 \mu\text{m}$ for temperatures higher than about 700 K. Radiative heat transfer is small compared with conduction for temperatures below 800 K in carbon preforms. Therefore, diffraction will be neglected in the following and a gray-body diffuse radiation model will be used.

Numerically, the perimeter of each fiber is discretized into facets (or faces). View-factors, which model the energy exchange between the faces, need to be calculated between the fiber faces:

$$F_{ij} = \frac{\text{Energy absorbed by face } A_j, \text{ by direct travel}}{\text{Diffuse energy emitted by face } A_i} \\ = \frac{1}{A_i} \int_{A_i} \int_{A_j} \frac{\cos(\theta_i) \cos(\theta_j)}{d^2} dA_i dA_j \quad (6)$$

which can be expressed both as an energy balance, or as a geometric quantity (isothermal facets). The view-factors are obtained using a collision-based Monte-Carlo method, to which reciprocity and least-squares closure is applied as described by Zeeb [9].

In the case of diffuse gray-body radiation, the radiosity of a face R_i , which is defined as the emitted energy of the face plus the portion of

the incoming radiation H_i that is reflected by the face, may be written as

$$R_i = \epsilon_\sigma \sigma T_i^4 + (1 - \epsilon_\sigma) H_i \quad (7)$$

By writing the energy balance equation for face i , as either the difference of the incident flux H_i and the total radiated flux R_i , or the absorbed flux and the emitted flux, we obtain the following:

$$q_i = H_i - R_i = \epsilon_\sigma H_i - \epsilon_\sigma \sigma T_i^4 \quad (8)$$

The incident flux on face i can be expressed by the sum of all the radiosities R_j , times the view-factors between facet i and the rest of the closed cavity

$$H_i = \sum_{j=1}^N R_j F_{ji} \quad (9)$$

Using reciprocity ($A_i F_{ij} = A_j F_{ji}$) and closure ($\sum_{j=1}^N F_{ij} = 1$) the final balance equation for facet i equals:

$$\sum_{j=1}^N F_{ij} (R_j - R_i) + \frac{\epsilon_\sigma}{1 - \epsilon_\sigma} (\sigma T_i^4 - R_i) = 0 \quad (10)$$

This formulation is known as the electrical analogy formulation for radiation heat exchange. It is described in detail by Modest [8]. The heat radiation equations are combined with the standard transient heat transfer equations for solids. This allows the modeling of the conduction and radiation problem in both transient and steady state. All the equations are implemented in the finite element code SAMCEF, which is used for industrial applications in the aerospace industry [10].

III. Steady-State Analysis

The goal of this analysis is to determine the effective radiative conductivity. For the steady-state analysis, the temperature on both sides of the model is imposed. This results in a known temperature difference ΔT over the model for a given mean temperature $T = (T_1 + T_2)/2$, T_1 and T_2 being the temperatures of the sides. This analysis is repeated for different temperatures T between 0 and 4000 K.

A. Test Matrix

The steady-state analysis is performed for five different configurations. All configurations have the same basic geometric layout (see Fig. 1), with a height Δy and a depth Δz of $100 \mu\text{m}$, but with different thicknesses. The model in Fig. 1 is a finite element model where every fiber is modeled using approximately 55 elements:

- 1) Configuration 1: 63 fibers with a length of $\Delta x = 0.5$ mm.
- 2) Configuration 2: 126 fibers with a length of $\Delta x = 1$ mm.
- 3) Configuration 3: 252 fibers with a length of $\Delta x = 2$ mm.
- 4) Configuration 4: 504 fibers with a length of $\Delta x = 4$ mm.
- 5) Configuration 5: 1008 fibers with a length of $\Delta x = 8$ mm.

All five configurations are generated in such a way that they have the same fiber volume fraction ($\approx 9.76\%$), resulting in an effective density ρ_0 of 175.68 kg/m^3 . For all configurations a total of five random geometries (seeds) are generated to assess the influence of the random fiber placement on the convergence of the solution.

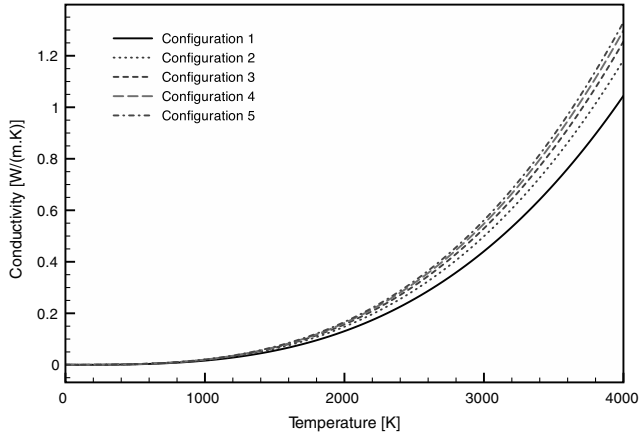


Fig. 2 Average effective conductivity λ_r as a function of temperature.

B. Effective Radiative Conductivity

The average effective conductivity curves for the five configurations are plotted in Fig. 2. As expected from the form of Eq. (2), the effective conductivity features an asymptotic behavior as a function of Δx . For all five configurations the values of k are presented in Table 1. The random nature of the geometry has very little effect of the value of k . In Fig. 3, the average \bar{k} values are plotted as a function of the model length Δx . The data are perfectly fitted using Eq. (3) with an extinction coefficient σ_{ext} of $63.11 \text{ m}^2/\text{kg}$.

IV. Transient Analysis

The objective of the transient analysis is to study the validity of the effective conductivity model in the transient regime. Two models are compared in this regime. The first one is the microscopic radiation model (direct numerical simulations at fiber scale). The second model is the classical macroscopic conduction model (conservation of enthalpy and Fourier's law for conduction). The goal is to test the validity in the transient regime using the approach developed in the previous section. As indicated in the paper of Marshall et al. [5], temperature-dependent effective conductivities are not expected to correctly model the thermal transient response of a porous material, especially in high heating-rate environments.

For the transient analysis we will reproduce the arc-jet heating environment test from Marshall et al. [5]. The model is initially at 300 K. The boundary condition is a time-dependent fixed temperature (Dirichlet) on one side of the sample and an adiabatic condition (Neumann) on the other side (see Fig. 4).

A. Test Matrix

Calculations are performed for two different values of Δx . For the effective heat transfer model, the material properties given in Table 2 are used. For the microscopic radiative model five runs are again performed to obtain averaged transient curves. For both the radiation and the equivalent model the temperature curves of five imaginary thermocouples were generated. The five imaginary thermocouples were positioned at the following places:

1) Thermocouple 1: positioned on the left-hand surface, where the temperature is imposed.

Table 1 Values of k for five random seeds

Configuration:	1	2	3	4	5
Seed	$k, -$				
1	0.798	0.432	0.233	0.121	0.062
2	0.785	0.445	0.233	0.121	0.062
3	0.761	0.447	0.238	0.122	0.061
4	0.796	0.447	0.232	0.122	0.062
5	0.758	0.435	0.236	0.121	0.062
\bar{k}	0.779	0.441	0.234	0.121	0.062

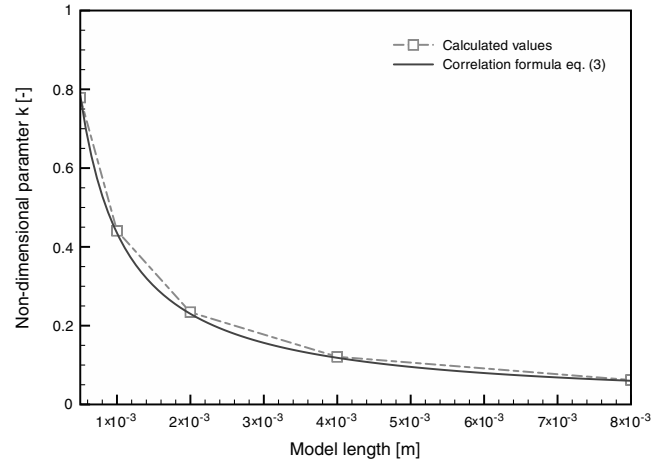


Fig. 3 \bar{k} -factor as a function of model length Δx .

- 2) Thermocouple 2: positioned at a depth of $\frac{1}{8} \Delta x$.
- 3) Thermocouple 3: positioned at a depth of $\frac{1}{4} \Delta x$.
- 4) Thermocouple 4: positioned at a depth of $\frac{1}{2} \Delta x$.
- 5) Thermocouple 5: positioned at the right hand surface.

For the microscopic radiation model, the thermocouples measure the average temperature of a group of elements (fibers). This approach is used because, at a given position, there might not be any fiber present.

B. Microscopic Radiation Model

For the transient radiation model, the temperature-dependent evolution of the enthalpy of the fibers is accounted for and the energy equation is solved for each fiber. The results shown in Fig. 4 are the

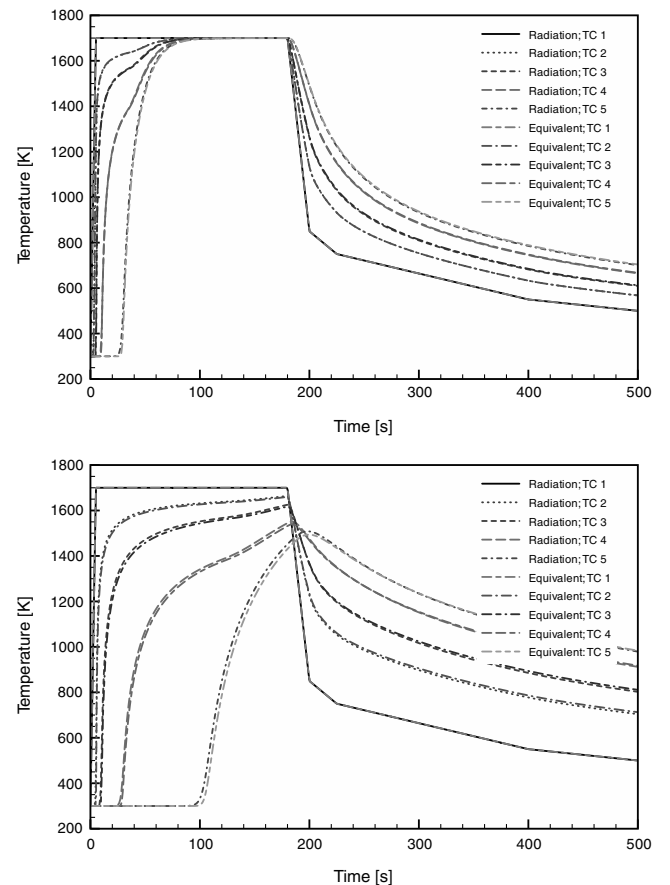


Fig. 4 Comparison of the temperature evolution for the effective macroscopic (equivalent) and the microscopic (radiation) models: a) calculation 1, and b) calculation 2.

Table 2 Effective conductivity properties

Calculation	Δx , m	ϵ_g , –	k , –	λ_r , W/(m.K)
1	$4 \cdot 10^{-3}$	0.85	$1.184 \cdot 10^{-1}$	$1.985 \cdot 10^{-11} \times T^3$
2	$8 \cdot 10^{-3}$	0.85	$6.000 \cdot 10^{-2}$	$2.012 \cdot 10^{-11} \times T^3$

averaged (five random geometries) results of the microscopic radiation model and the results of the equivalent macroscopic model. It is interesting to notice that the thermocouple curves 2, 3, and 4 show a distinctive *bend* in the high temperature range (at $t \approx 120$ s). The reason for this bend is not directly obvious from looking at the full radiation equations, but the effective conductivity Eq. (4) is more explicit. As can be seen from this equation, the heat flux q_r depends on both ΔT and T^3 . As a consequence at the beginning of the analysis ΔT is high and the structure heats up quickly. This effect will eventually level off but is taken over in the high temperature range by the T^3 term.

C. Effective Macroscopic Conductivity Model

The macroscopic model consists of a uniform mesh with a total length of Δx , with a material effective density of 175.68 kg/m^3 . We use the effective conductivities reported in Table 2. The results of the macroscopic calculation and the radiation calculation are shown in Fig. 4. The macroscopic calculation reproduces the DNS results accurately, even during the high heating-rate transient phase.

V. Conclusions

Direct numerical simulations of the radiation heat transfer in two-dimensional fibrous media have enabled the validation of a semi-analytical (phenomenological) model for the effective radiative conductivity. The effective conductivity is shown to be a function of three parameters: the local temperature T^3 , the extinction coefficient, and the sample thickness. The extinction coefficient of a two-dimensional fiber preform, made of randomly positioned but parallel fibers, has been determined by inverse analysis in steady state. Transient regime simulations have been carried out using both DNS and a macroscopic model for heat transfer (Fourier's law). When the effective radiation conductivity computed in steady state (using DNS) is used as an input to the macroscopic model, the macroscopic

model correctly reproduces the DNS, at least at the heating rates tested here. Hence, the results from our study indicate that the proposed correlation can be used for both steady-state and transient analysis. The results show that the Rosseland hypothesis used to linearize the radiative heat transfer is valid in the studied case.

References

- [1] Lee, S. C., "Radiation Heat-Transfer Model for Fibers Oriented Parallel to Diffuse Boundaries," *Journal of Thermophysics and Heat Transfer*, Vol. 2, 1988, pp. 303–308.
doi:10.2514/3.104
- [2] Petrov, V. A., "Combined Radiation and Conduction Heat Transfer in High Temperature Fiber Thermal Insulation," *International Journal of Heat and Mass Transfer*, Vol. 40, No. 9, 1997, pp. 2241–2247.
doi:10.1016/S0017-9310(96)00242-6
- [3] Lee, S. C., and Cunningham, G. R., "Conduction and Radiation Heat Transfer in High-Porosity Fiber Thermal Insulation," *Journal of Thermophysics and Heat Transfer*, Vol. 14, 2000, pp. 121–136.
doi:10.2514/2.6508
- [4] Banas, R. P., and Cunningham, G. R., "Determination of the Effective Thermal Conductivity for the Space Shuttle Orbiter's Reusable Surface Insulation," AIAA Paper 1974-730, July 1974.
- [5] Marschall, J., Maddren, J., and Parks, J., "Internal Radiation Transport and Effective Thermal Conductivity of Fibrous Ceramic Insulation," AIAA Paper 2001-2822, June 2001.
- [6] Bankvall, C., "Heat Transfer in Fibrous Materials," *Journal of Testing and Evaluation*, Vol. 1, No. 3, 1973, pp. 235–243.
doi:10.1520/JTE10010J
- [7] Deissler, R. G., "Diffusion Approximation for Thermal Radiation in Gases with Jump Boundary Condition," *Proceedings of the ASME-AIChE Heat Transfer Conference*, ASME Paper 63-HT-13, 1963.
- [8] Modest, M. F., *Radiative Heat Transfer*, 2nd ed., McGraw-Hill, New York, 1993.
- [9] Zeeb, C., "Performance and Accuracy Enhancements of Radiative Heat Transfer Modeling via Monte-Carlo," Ph.D. Thesis, Colorado State Univ., 2002.
- [10] Plotard, P., and Labaste, V., "Entry System Development for Mars Netlander Mission," *Acta Astronautica*, Vol. 55, Nos. 3–9, 2004, pp. 677–686.
doi:10.1016/j.actaastro.2004.05.059

G. Palmer
Associate Editor